JACC: CARDIOVASCULAR IMAGING VOL. 8, NO. 2, 2015

ISSN 1936-878X/$36.00
PUBLISHED BY ELSEVIER INC. http://dx.doi.org/10.1016/j.jcmg.2014.12.005

iREVIEWS

STATE-OF-THE-ART PAPERS

OCT for the Identification of Vulnerable Plaque in Acute Coronary Syndrome

Hannah Sinclair, MB, ChB,*† Christos Bourantas, MD, PhD,† Alan Bagnall, MB, ChB, PhD,† Gary S. Mintz, MD,‡ Vijay Kunadian, MBBS, MD*†

ABSTRACT

After 2 decades of development and use in interventional cardiology research, optical coherence tomography (OCT) has now become a core intravascular imaging modality in clinical practice. Its unprecedented spatial resolution allows visualization of the key components of the atherosclerotic plaque that appear to confer "vulnerability" to rupture—namely the thickness of the fibrous cap, size of the necrotic core, and the presence of macrophages. The utility of OCT in the evaluation of plaque composition can provide insights into the pathophysiology of acute coronary syndrome and the healing that occurs thereafter. A brief summary of the principles of OCT technology and a comparison with other intravascular imaging modalities is presented. The review focuses on the current evidence for the use of OCT in identifying vulnerable plaques in acute coronary syndrome and its limitations. (J Am Coll Cardiol Img 2015;8:198–209)

Optical coherence tomography (OCT) is an intravascular imaging modality that uses the reflection of near-infrared light to generate an image. OCT was first described more than 2 decades ago when it was used to image the peripapillary area of the human retina in vitro (1). Eleven years later, OCT was used to image atherosclerotic plaques in human coronary arteries (2). The image resolution achievable with OCT (axial: 10 μm, lateral: 20 to 40 μm) far surpasses that of intravascular ultrasound (IVUS) (100 to 200 μm). Histological studies have shown that certain adverse plaque phenotypes are associated with the onset of an acute coronary syndrome (ACS) (3). With its excellent spatial resolution, OCT is ideally placed to identify vulnerable plaque that could result in ACS.

This review describes the technology underlying OCT, its potential for identifying vulnerable plaques in ACS, and its limitations.

OCT TECHNOLOGY

To generate an image, a low-coherence, near-infrared (wavelength of 1.3 μm) light source is directed at the tissue (**Figure 1**). The light beam is split into 2 arms, a sample arm and a reference arm, by an interferometer. The reference arm is directed to a mirror, which reflects the light directly back to the interferometer. The light of the sample arm is absorbed, refracted, or reflected from the sample tissue, scattering the light at large angles from its surface and sub-surface. Reflected light travels back to the interferometer and

From the *Institute of Cellular Medicine, Faculty of Medical Sciences, Newcastle University, Newcastle upon Tyne Hospitals NHS Foundation Trust, Newcastle upon Tyne, United Kingdom; †Cardiothoracic Centre, Freeman Hospital, Newcastle upon Tyne Hospitals NHS Foundation Trust, Newcastle upon Tyne, United Kingdom; and the ‡Cardiovascular Research Foundation, New York, New York. The research is supported by the National Institute for Health Research (NIHR) Newcastle Biomedical Research Centre based at Newcastle upon Tyne Hospitals NHS Foundation Trust and Newcastle University. The views expressed are those of the authors and not necessarily those of the NHS, the NIHR or the Department of Health. All of the authors have reported that they have no relationships relevant to the contents of this paper to disclose.

Manuscript received October 14, 2014; revised manuscript received December 4, 2014, accepted December 9, 2014.

interacts with the reference arm light. The interaction between these 2 light waves determines the OCT image, depending on whether there is constructive or destructive interference between the waves (1). Because red blood cells strongly scatter the light waves and hence attenuate the image, OCT requires a bloodless field. The OCT catheter is connected to a rotary junction, which uses a motor to rotate the optical fiber in the catheter and couples light from this rotating fiber to light from the reference arm. The rotary junction is mounted to an automated pullback device, thus scanning the artery in a helical fashion.

There are 2 types of OCT systems: time domain (**Figure 1A**) and frequency domain (**Figure 1B**). The first-generation time domain–OCT system required sequential measurement of optical echoes from different depths by moving the reference mirror (4). This initially required the use of a balloon to occlude coronary blood flow, and the slow pullback speed of 1 to 5 mm/s led to image acquisition times of 3 to 45 s (4). Subsequently, a blood-free imaging field was obtained by controlled intracoronary infusion of isoosmolar contrast, negating the need for an occlusive balloon (5). This reduced the procedure time, although the length of the analyzed segments of artery were shorter (5). Second-generation frequency domain–OCT systems use a light source that is rapidly swept in time across wavelengths from 1.25 to 1.35 μm, allowing simultaneous recording of reflections from different depths without movement of the reference mirror (6). Depth profiles are then reconstructed by Fourier transformation. This speeds up image acquisition 10-fold, with achievable pullback speeds of up to 40 mm/s and imaging runs of up to 150 mm in length with a 3- to 5-s flush of saline or contrast, without the need for prolonged vessel occlusion (6).

OCT IMAGE FEATURES. The normal coronary artery is seen as a 3-layered structure on OCT (**Figure 2A**) (7). The internal elastic lamina appears as a signal-rich 20-μm-thick band that lies inside the dark band of the media and the further signal-rich band of the external elastic lamina (7). An atherosclerotic lesion is seen on OCT as a mass lesion within the arterial wall, with focal intimal thickening or loss of the normal vessel architecture (8). Fibrous plaque produces a relatively homogenous and highly backscattering signal (8) (**Figure 2B**). Calcified plaques appear as a signal-poor area with sharply delineated borders (**Figure 2C**). However, this only applies to larger regions of calcification; smaller areas and microcalcifications have yet to be validated against histology (8). Necrotic core (and the broader histopathological category of a lipid pool) is seen as a signal-poor region with poorly defined borders and fast OCT signal drop-off (**Figure 2D**) (8). Because light does not penetrate through these areas, OCT cannot be used to measure the depth or volume of lipid pools. Macrophage accumulations can sometimes be seen at the border of the fibrous cap and necrotic core, and can appear as punctate signal-rich spots that exceed the background noise of the image (8). Cholesterol crystals are linear regions of high intensity, often associated with a lipid pool (**Figure 3C**) (8). OCT can differentiate between white and red thrombus (**Figure 4**) due to the high proportion of red blood cells in red thrombi, which causes greater attenuation of the OCT signal and a lower half-width (the distance from peak signal intensity to its half-intensity). Kume et al. (9) showed that a cutoff of 250 μm in the half-width could accurately discriminate between white and red thrombus with a sensitivity of 90% and a specificity of 88%.

HISTOLOGICAL VALIDATION OF OCT. OCT was first validated for plaque characterization in vitro in 2002 (10). Agreement between the histopathological and OCT findings were high ($\kappa = 0.83$ to 0.84), and interobserver and intraobserver reliability were good ($\kappa = 0.88$ and $\kappa = 0.91$, respectively) (10). However, there were a number of false-negative diagnoses of lipid pools, which could be attributed to the limited penetration of OCT, leading to deep lipid pools being misinterpreted as fibrous plaques. Intimal thickness measured by OCT also correlated well with histology ($r = 0.98$, $p < 0.001$) (11). However, OCT images are prone to artifacts; 30.9% of images contained artifacts in 1 study, although this improved with operator experience (12). Seam-line artifacts cause apparent breaks in the lumen contour on the cross-sectional image (6.0% of images); decentration artifacts are caused by eccentric positioning of the imaging catheter within the artery and lead to image attenuation in remote structures (30.9%); caliber artifacts are caused by an arterial diameter greater than the penetration limit of the OCT and are a particular problem in vein grafts and in the left main stem (13) (15.0%); and flow artifacts are caused by failure to clear blood from either the vessel or imaging catheter by flushing (19.6%) (12).

OCT AND VULNERABLE PLAQUES

DEFINITION OF THIN-CAP FIBROATHEROMA. Histopathological studies have identified anatomical characteristics of "vulnerable" plaques that are

ABBREVIATIONS AND ACRONYMS

ACS = acute coronary syndrome

CKD = chronic kidney disease

DM = diabetes mellitus

IVUS = intravascular ultrasound

NIRS = near-infrared spectroscopy

OCT = optical coherence tomography

SCAD = spontaneous coronary artery dissection

STEMI = ST-segment elevation myocardial infarction

TCFA = thin-cap fibroatheroma

FIGURE 1 Diagrammatic Representation of OCT

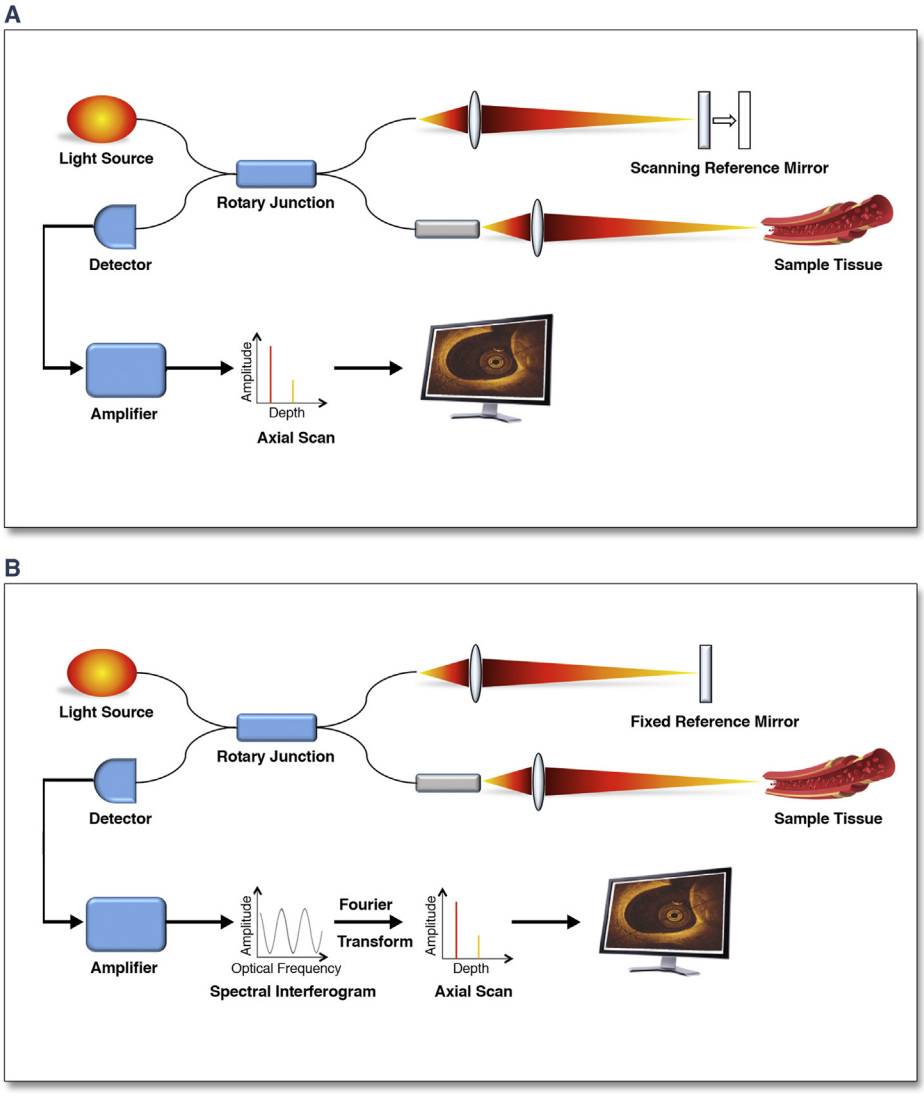

The 2 types of optical coherence tomography (OCT) systems, **(A)** time domain and **(B)** frequency domain, are displayed.

implicated in the pathophysiology of ACS. These plaques, which are prone to rupture, have fibrous caps that are thinned and rich in macrophages overlying a lipid pool (14). A previous study examined the hearts of 113 men that died suddenly, of which 41 had acute coronary artery thrombosis secondary to rupture of an atherosclerotic plaque, and 95% of these subjects had plaques with fibrous caps <65-μm thick (mean thickness, 23 ± 19 μm) with an infiltrate of macrophages (15), subsequently termed thin-cap fibroatheroma (TCFA) (16). Due to the high image resolution with OCT, it is well placed to identify these high-risk plaques in vivo (**Figure 5**). However, there is still debate over the exact definition of a TCFA on OCT (OCT-TCFA) because histological specimens of TCFA differ from OCT images (likely due to shrinkage of pathological specimens). Using a cutoff of 70 μm (as the axial resolution of OCT is >10 μm), only 67% of ruptured plaques in 1 study of 72 patients with ACS were defined as having a thin fibrous cap (17). Therefore, it is possible that the fibrous cap of a TCFA is thicker in vivo than on histology. There is a higher proportion of lipid-rich plaque on OCT in patients with ACS compared with stable angina (18), and some studies have used an additional parameter to define a TCFA: that the arc of the lipid pool should subtend an

FIGURE 2 **OCT Image Examples of Plaque Composition**

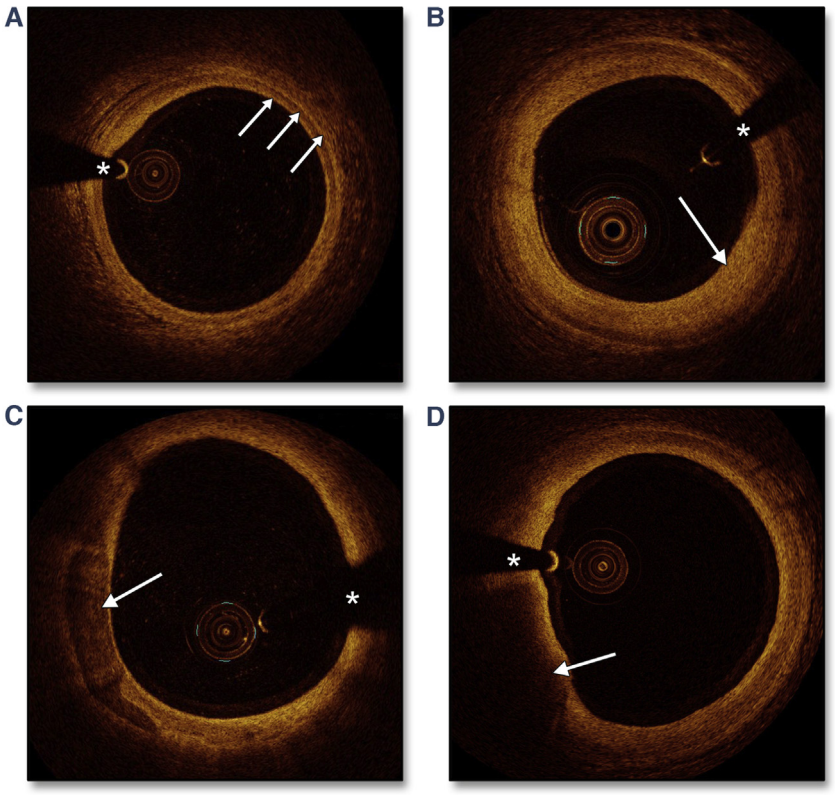

(A) Composition of the normal coronary artery, with **white arrows** depicting the internal elastic lamina, media and external elastic lamina. **(B)** Concentric fibrous plaque. **(C)** Calcified plaque. **(D)** Necrotic core. *Guidewire artifact. Abbreviation as in **Figure 1**.

angle >90° (8). However, there is no consensus on the exact cutoff value for the fibrous cap or arc of lipid pool for the identification of an OCT-TCFA, only that the definition of an OCT-TCFA should reflect the histological definition of a TCFA (8).

TCFA IN ACS. TCFAs are more common in patients with an acute or unstable clinical presentation than stable angina pectoris patients. A comparison of 26 acute ST-segment elevation myocardial infarction (STEMI) patients with 16 stable angina patients showed that STEMI patients had a higher proportion of OCT-TCFA in the culprit lesion (85% vs. 13%, $p < 0.001$) and a thinner fibrous cap (57 ± 12 μm vs. 180 ± 65 μm, $p < 0.001$) (19). Patients with STEMI also had a higher prevalence of OCT-TCFA compared with patients with non–ST-segment elevation ACS (78% vs. 49%, $p = 0.008$) (20). Similar results have been shown in patients with unstable angina compared to patients with stable angina (incidence of OCT-TCFA 81% vs. 47%, $p = 0.002$; fibrous cap thickness of 56 ± 20 μm vs. 75 ± 30 μm, $p < 0.001$) (21). Patients with ACS also have a higher proportion of OCT-TCFA and thinner fibrous caps than found in non-ACS patients (19,22). In patients with ACS, OCT-TCFAs are more commonly found in the proximal segments of the culprit vessel (23,24). OCT has been used to confirm findings from histological studies that plaque rupture of TCFA occurs more often away from the site of minimum lumen area in patients with STEMI and non-STEMI (mean distance of site of rupture from minimum lumen area = 2.34 ± 2.31 mm) (25).

Atherosclerotic lesions are dynamic, and there is evidence from IVUS studies that TCFAs can transform into other plaque types and vice versa. A study of nonculprit lesions in patients with STEMI showed that 9 of 41 TCFAs identified by virtual histology-IVUS had healed into more stable lesions at 13-month follow-up, but 21 of 57 other lesions had transformed into TCFAs (26). However, in a study evaluating bifurcation lesions with both OCT and virtual histology-IVUS, 83% of high-risk plaques remained unchanged at 6 months (27). Further serial OCT studies are required to investigate the natural history of these vulnerable plaques in patients with ACS.

FIGURE 3 Cholesterol Crystals

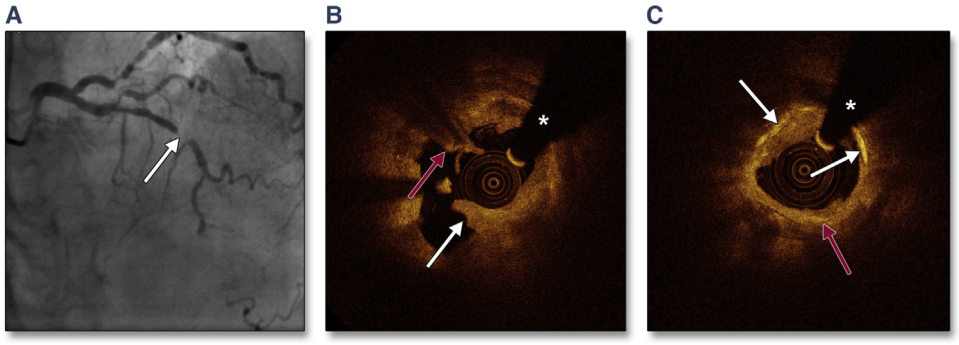

Images from an 80-year-old female patient with hypertension and hypercholesterolemia who presented with a non–ST-segment elevation myocardial infarction. **(A)** Angiogram showing a tight stenosis with thrombus in the mid-left anterior descending artery **(white arrow). (B)** OCT image of red **(red arrow)** and white **(white arrow)** thrombus in the culprit lesion. **(C)** OCT image of cholesterol crystals **(white arrows)** and macrophage accumulation **(red arrow)**. *Guidewire artifact. OCT = optical coherence tomography.

EFFECTS OF THERAPY ON TCFA. Methods to stabilize these vulnerable TCFAs have been assessed using serial OCT studies. Patients who underwent statin therapy had an increased cap thickness of OCT-TCFA compared with patients who were not being administered statins (an increase of 192 ± 41 μm vs. 25 ± 8 μm, $p < 0.001$) at 9 months post-ACS study (28). In a prospective study of 42 patients with stable angina, statin therapy resulted in an increase in fibrous cap thickness when compared with dietary modification alone (+52 ± 32 μm vs. 2 ± 22 μm, $p < 0.001$) (29). Another study enrolled 30 patients (56.6% with ACS) with untreated dyslipidemia and OCT-TCFA on baseline imaging, and randomized them to either statin therapy alone or statin + eicosapentaenoic acid (30). Despite similar levels of low-density lipoprotein at follow-up examination, those who received eicosapentaenoic acid had a greater increase in fibrous cap thickness (54.8 ± 27.9 μm vs. 23.5 ± 11.6 μm, $p < 0.0001$) (30). However, it remains to be seen whether stabilizing these plaques actually improves clinical outcomes.

FIGURE 4 Red and White Thrombus

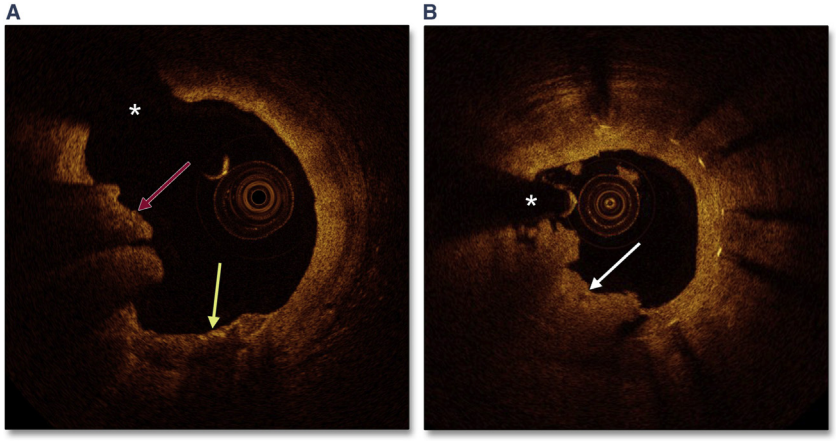

(A) Red thrombus **(red arrow)** with high attenuation, associated with a calcified plaque **(yellow arrow). (B)** Stent thrombosis with homogenous, low-attenuation white thrombus **(white arrow)**. *Guidewire artifact.

FIGURE 5 Thin-Cap Fibroatheroma

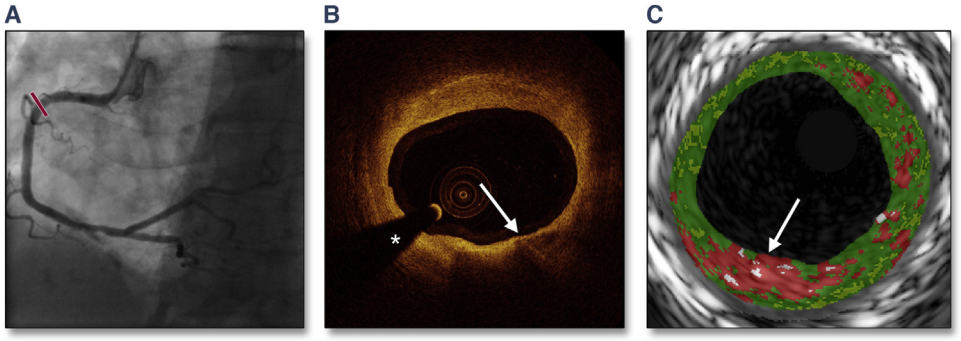

Images from an 83-year-old male ex-smoker, who presented with a non-ST-segment elevation myocardial infarction. He underwent percutaneous coronary intervention to a culprit lesion in the left anterior descending artery, but OCT imaging of the right coronary artery revealed a nonobstructive thin-cap fibroatheroma in the nonculprit artery. **(A)** Angiogram with a nonobstructive mild atheroma in the right coronary artery **(red bar)**. **(B)** OCT image of the thin-cap fibroatheroma **(white arrow)**. **(C)** VH-IVUS image of the thin-cap fibroatheroma **(white arrow)**. *Guidewire artifact. OCT = optical coherence tomography; VH-IVUS = virtual histology–intravascular ultrasound.

RUPTURED PLAQUES. Ruptured plaques with thrombus have thinner fibrous caps than those without thrombus (57 ± 17 μm vs. 96 ± 48 μm, p = 0.0076) (31). Intracoronary thrombus is well visualized by OCT and is almost universally found in STEMI (19). However, care must be taken with interpretation of these results, as overlying thrombus may interfere with OCT characterization of the lesion, and performing thrombus aspiration before OCT imaging may alter the underlying plaque anatomy. Patients with ACS caused by ruptured culprit plaques are more likely to have nonculprit plaques with a higher lipid index (mean lipid arc multiplied by lipid length measured in the longitudinal view: 1,196.9 ± 700.5 vs. 747.7 ± 377.3, p = 0.001), higher incidence of OCT-TCFA (52.9% vs. 19.0%, p = 0.029), and thinner fibrous caps (107.0 ± 56.5 mm vs. 137.3 ± 69.8 mm, p = 0.035) on OCT than those with nonruptured culprit plaques (32). Patients with ruptured culprit plaques were also more likely to have secondary, nonculprit plaques ruptures (35.3% vs. 4.8%, p = 0.016) (32). This suggests that these patients have increased pan-coronary vulnerability and may be at higher risk of future adverse events. In addition, plaque ruptures in patients with ACS differ from those found in patients with asymptomatic coronary artery disease with a greater lipid arc (171 ± 71° vs. 133 ± 71°, p = 0.037), higher incidence of thrombus (78% vs. 9%, p < 0.001), and a smaller minimum lumen area of the culprit lesion (1.79 ± 0.92 mm vs. 2.75 ± 0.99 mm, p < 0.001), suggesting that the morphology of the plaque rupture may influence whether it heals asymptomatically or causes an adverse cardiovascular event (33).

PLAQUE EROSION. In contrast to plaque rupture, plaque erosion is characterized by luminal thrombus and absence of the endothelium, without evidence of fibrous cap disruption (3). In 1 histological study, erosions were responsible for more than 40% of thrombotic sudden cardiac deaths and were more prevalent in women (14). Although OCT does not have the resolution necessary to identify the absence of the endothelium, OCT-identified plaque erosion has been defined as the presence of thrombus and an irregular luminal surface in the absence of cap rupture (8). In a cohort of patients with STEMI (n = 30), plaque erosions were more often found by OCT than by IVUS or angioscopy (23% vs. 3% vs. 0%, p = 0.003) (34). In a previous study, OCT was performed in 126 patients with ACS and showed plaque rupture in 43.7%, erosions in 31%, and calcified nodules in 7.9% (35). Plaque erosions were more commonly observed in younger patients (53.8 ± 13.1 years vs. 60.6 ± 11.5 years, p = 0.005), and were more commonly associated with non-STEMI than STEMI (61.5% of patients with non-STEMI had a plaque erosion vs. 29.1% of STEMI patients, p = 0.008). Patients with plaque erosion had a less severe diameter culprit stenosis than those with plaque rupture (55.4 ± 14.7% vs. 68.8 ± 12.9%, p < 0.001) (35). Plaque erosion on OCT was associated with a higher level of serum myeloperoxidase, a hemoprotein released on neutrophil activation, than plaque rupture (2,500 ng/ml vs. 707 ng/ml, p = 0.001) (36).

Prati et al. (37) performed OCT after thrombus aspiration in patients with STEMI and followed up 31 patients with plaque erosion for 1 year. Twelve

patients were managed with thrombus aspiration only, and 19 had thrombus aspiration plus angioplasty. There were no significant differences in outcomes (death, myocardial infarction, and target vessel revascularization) between the groups (37). Although this study raised the possibility of using OCT to influence the management of patients with ACS, this study is limited in that it consisted of too small a sample size to draw definitive conclusions, and treatment was not randomized (patients managed conservatively were younger and had fewer cardiac risk factors).

PLAQUES WITH CALCIFIED NODULES. Plaques with superficial calcified nodules are also considered prone to rupture (16,38). The pattern of plaque calcification on OCT was evaluated in 187 patients with acute myocardial infarction and unstable and stable angina. Patients with acute myocardial infarction and unstable angina had less overall calcium (measured by arc, area, and length, $p < 0.001$ for all measurements) than those with stable angina, but were more likely to have spotty calcium deposits closer to the surface of the plaque (39). The incidence of calcified nodules in ACS in 1 study was 8%, but was more common with increasing age (35). However, the accuracy of OCT in identifying smaller areas of calcification has also yet to be validated against histology (8).

MACROPHAGE INFILTRATION AND MICROCHANNEL FORMATION. The resolution of OCT may allow identification of macrophages within an atherosclerotic plaque. In ACS patients, a higher prevalence of macrophage infiltration in nonculprit plaques was found compared with non-ACS patients (82.4% vs. 37.9%, $p = 0.001$) (22). A study of diabetic patients also found those with poorly controlled diabetes (glycated hemoglobin ≥ 8%) had greater macrophage infiltration than nondiabetic patients or well-controlled diabetic patients (37.9% vs. 11.0%, $p = 0.037$) (40). Plaques that exhibited an increase in luminal stenosis over time were more likely to have higher numbers of macrophages (odds ratio [OR]: 9.6, $p = 0.001$), TCFA (OR: 20, $p < 0.001$), intimal laceration (OR: 10.2, $p < 0.001$), and/or microchannels (OR: 20, $p < 0.001$) (41). Plaque neovascularization and microchannel formation (**Figure 6**) are known to be markers of plaque vulnerability and rupture, as well as intraplaque hemorrhage, which can contribute to plaque progression (42). Patients with microchannels in the culprit lesion were more likely to have presented with unstable than stable angina (83% vs. 17%), have a thinner fibrous cap (60 μm vs. 100 μm, $p = 0.001$), and have a trend towards a higher incidence of plaque rupture (50% vs. 28%, $p = 0.11$) (43).

FIGURE 6 Microchannel

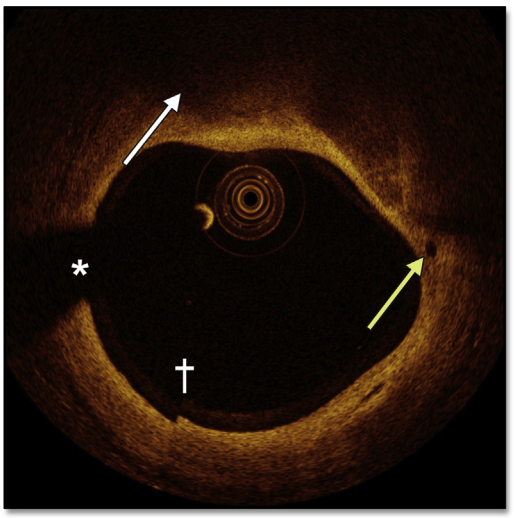

OCT image showing a microchannel **(yellow arrow)** associated with a nonobstructive lesion with a large necrotic core **(white arrow)**. *Guidewire artifact. †Seam line artifact. OCT = optical coherence tomography.

COMPARISON WITH OTHER INTRAVASCULAR MODALITIES

Table 1 shows the properties of the different available clinical intravascular imaging modalities. A combination of these imaging techniques may provide a more detailed and complete visualization of plaque pathology.

INTRAVASCULAR ULTRASOUND. Because of its greater resolution and obligatory flushing and blood clearing, OCT is more accurate than either IVUS or quantitative coronary angiography in determining luminal dimensions (44). Frequency domain–OCT provides more accurate measurement of the minimal lumen area than either IVUS or quantitative coronary angiography in both phantom models and in vivo ($r^2 = 0.95$, $p < 0.001$, mean difference 0.41 mm^2) with good intra- and interobserver reproducibility ($r^2 = 0.999$, $p < 0.001$, mean difference 0.01 mm^2) (44). Virtual histology–IVUS cannot visualize the fibrous cap but can quantify the necrotic core of the plaque (**Figure 5C**) (45). Virtual histology–IVUS was shown to have acceptable sensitivity (89%) and specificity (86%) in identifying TCFA compared with OCT (46). A hybrid IVUS–OCT catheter has been developed and simultaneously provides both the resolution and penetration required to identify and quantify TCFA (47,48).

TABLE 1 Comparison of the Physical Properties of Different Modalities of Intravascular Imaging

	OCT	IVUS	Near-Infrared Spectroscopy
Energy source	Infrared	Ultrasound	Near-infrared
Wavelength (μm)	1.3	35–80	0.8–2.5
Penetration (mm)	1–2.5	10	1–2
Resolution (μm)	20–40	100–200	NA
Pullback speed (mm/s)	10–40	0.5–1	0.5

IVUS = intravascular ultrasound; NA = not available; OCT = optical coherence tomography.

FRACTIONAL FLOW RESERVE. Although OCT is a structural imaging technique, there have been attempts to correlate it with functional measures of stenosis severity, such as fractional flow reserve. Table 2 summarizes the studies that have correlated minimum lumen area (measured by OCT) and fractional flow reserve. The ILUMIEN 1 study is currently recruiting to ascertain whether a combined OCT and fractional flow reserve device aids periprocedural decision making that may have an impact on patient outcomes (49).

NEAR-INFRARED SPECTROSCOPY. Near-infrared spectroscopy (NIRS) can only quantify the lipid content of the plaque, but the signal can pass through calcium and accurately quantify lipid behind this (50). NIRS provides only compositional information regarding the plaque, but does not require a bloodless field (51) and can help discriminate between calcium and necrotic core, which can often be misinterpreted on OCT (52). A comparison using a hybrid NIRS-IVUS catheter with OCT showed that plaque burden, positive remodeling, and lipid index measured by the hybrid catheter were associated with OCT-TCFA (53). A hybrid NIRS-OCT catheter is in development, and a proof-of-concept demonstration has been published, successfully imaging a 3-cm section of 1 human coronary artery ex vivo to provide simultaneous structural and compositional information (54).

3-DIMENSIONAL RECONSTRUCTION. As the technology of OCT becomes more refined and image acquisition faster, it has become possible to perform 3-dimensional reconstructions of the coronary anatomy by fusing x-ray and OCT data (55,56). This allows assessment of local hemodynamic flow patterns and hence the effects of endothelial shear stress on the risk of plaque progression and rupture (57). Three-dimensional IVUS studies have shown that localized elevation of shear stress is correlated with the plaque rupture site in patients with ACS ($\kappa = 0.79$) (58). However, this has not yet been studied using OCT.

NONINVASIVE IMAGING. Noninvasive techniques such as positron emission tomography–computed tomography have been used to identify vulnerable plaques and correlate with high-risk features on virtual histology–IVUS. In 40 patients with stable angina, high ^{18}F-sodium fluoride uptake (postulated to be a marker of plaque activity) correlated with virtual histology–IVUS features such as microcalcification (73% vs. 21%, p = 0.002) and higher mean necrotic core (24.6 vs. 18.0, p = 0.001), which may be markers of plaque vulnerability, and there was a nonsignificant trend towards a higher prevalence of TCFA in ^{18}F-sodium fluoride positive plaques (47% vs. 16%, p = 0.068) (59). However, these noninvasive techniques lack the spatial resolution of OCT, and it has not yet been investigated whether OCT can complement the data obtained from positron emission tomography–computed tomography.

OTHER APPLICATIONS OF OCT

NEOATHEROSCLEROSIS. The advent of OCT has allowed in vivo imaging of conditions that were

TABLE 2 Summary of Studies Comparing FFR and OCT

First Author, Year (Ref. #)	Lesions Assessed	Type of OCT	FFR	MLA Cutoff	Positive Predictive Value	Negative Predictive Value	Sensitivity	Specificity
Zafar et al., 2014 (88)	N = 41 >30% stenosis	FD-OCT	<0.80	<1.62 mm^2	89%	91%	97%	70%
Reith et al., 2013 (89)	N = 62 40%–70% stenosis Diabetic patients	FD-OCT	<0.80	<1.59 mm^2	80.6%	74.2%	75.8%	79.3%
Pyxaras et al., 2013 (90)	N = 55 30%–50% stenosis	FD-OCT	<0.80	<2.88 mm^2	Not reported	Not reported	73%	71%
Pawlowski et al., 2013 (91)	N = 48 40%–70% stenosis	Non-occlusive TD-OCT	<0.80	<2.05 mm^2	Not reported	Not reported	75%	90%
Gonzalo et al., 2012 (92)	N = 61 40%–70% stenosis	FD-OCT	<0.80	<1.95 mm^2	66%	80%	83%	63%
Shiono et al., 2012 (93)	N = 62 >30% stenosis	Occlusive TD-OCT	<0.75	<1.91 mm^2	80.6%	92.3%	93.5%	77.4%

FD-OCT = frequency domain optical coherence tomography; FFR = fractional flow reserve; MLA = minimum lumen area; OCT = optical coherence tomography; TD-OCT = time domain optical coherence tomography.

previously poorly understood. In-stent restenosis was previously thought to be a condition mainly of bare-metal stents that regressed with time (60). However, more recently, evidence has emerged of late in-stent restenosis of both bare-metal and drug-eluting stents presenting as ACS (61,62). An early OCT study of in-stent restenosis in bare-metal stents showed that the initial neointimal proliferation after stent implantation could transform into lipid-rich plaque with evidence of intimal disruption and thrombus (63). TCFAs were identified in more than one-half of drug-eluting stent restenosis cases, and features of neoatherosclerosis were more common in those presenting with unstable angina than those patients with stable symptoms (64). In 1 serial OCT study of drug-eluting stents, 30.3% of those with homogenous neointimal proliferation had evidence of transformation to neoatherosclerosis (65). On multivariate analysis, stent age >4 years, chronic kidney disease (CKD), and smoking were predictors for neoatherosclerosis on OCT (66). Neoatherosclerosis is also observed more often in patients with diabetes mellitus (DM), and more often in poorly controlled DM (67). Patients with neoatherosclerosis have a higher rate of target vessel revascularization and stent thrombosis (68).

SPONTANEOUS CORONARY ARTERY DISSECTION. OCT can also provide a valuable insight into less common causes of ACS, such as spontaneous coronary artery dissection (SCAD) and coronary artery spasm. SCAD is a non-traumatic, spontaneous separation of the vessel wall by intramural hemorrhage, with creation of a false lumen, and may be easily missed on angiography (69). OCT is advocated as the gold-standard intravascular imaging modality in detecting SCAD because it can visualize the false lumen, intimal rupture, and intramural thrombus more accurately than IVUS (70). In 17 patients suspected of having SCAD, OCT confirmed its presence in 11 (64.7%), showing a double lumen or intramural hemorrhage in all patients, whereas angiography only showed an intimal flap in 3 patients (71). SCAD was observed in 4% of cases in a recent ACS cohort, and was more common in women than men (72). A diagnostic algorithm has been proposed if there is a high index of suspicion of SCAD (for example, in a young woman without traditional risk factors presenting with ACS), advocating the use of OCT or IVUS to confirm the diagnosis (69).

CORONARY ARTERY SPASM. Coronary artery spasm (mediated by endothelial dysfunction and atheroma that is not visible on conventional angiography) can also result in ACS, and 1 OCT study of 20 patients with coronary vasospasm (confirmed by provocation testing) showed intraluminal thrombus and intimal erosion in a significant proportion of cases (33.3% and 10%, respectively) (73). One study showed that patients with coronary artery spasm after an acetylcholine provocation test were more likely to have homogenous intimal thickening than those without coronary spasm (74). However, another OCT study suggested that contraction of the media facilitated intimal gathering without intimal thickening during coronary artery spasm (75). Further research is needed into the pathophysiology of coronary artery spasm, and OCT is ideally placed to identify the role of plaque erosion and changes in the intima during spasm.

OCT PLAQUE CHARACTERIZATION IN VULNERABLE PATIENTS

DIABETES MELLITUS. Patients with DM are at increased risk of adverse events after ACS (hazard ratio for cardiac death at 1 year was 3.33, 95% confidence interval: 1.3 to 8.6, $p = 0.008$) (76). However, studies have shown a similar prevalence of TCFA in DM and non-DM patients undergoing angioplasty for any reason (29% in patients with DM vs. 36% in those without, $p = 0.76$) (77), and in patients with unstable angina (42.9% vs. 52.3%, $p = 0.34$) (78). In an OCT substudy of 72 patients with ACS, patients with DM had smaller lipid pools, greater extent of calcification, and a greater frequency of superficial calcified nodules, with no difference in the prevalence of TCFA between groups (79). Features of plaque vulnerability are, however, associated with glycemic control in diabetic patients, with patients with a glycated hemoglobin level ≥8% found to have a larger lipid pool, thinner fibrous cap, and greater prevalence of TCFA in nonculprit lesions (40).

RENAL DYSFUNCTION. Ischemic heart disease is the leading cause of death in patients with CKD (80). In a study of 287 patients enrolled in the Massachusetts General Hospital OCT Registry (26.5% with ACS), patients with CKD had a larger lipid index compared with those without (average lipid arc multiplied by lipid length: 1,716.1 ± 1,116.2 mm vs. 1,248.4 ± 782.8 mm, $p = 0.003$) (81). Plaque disruption was more frequently found in the CKD than the non-CKD group (13.5% vs. 5.5%, $p = 0.049$), but there were no differences in fibrous cap thickness between the groups (81).

CARDIAC ALLOGRAFT VASCULOPATHY. OCT has been used in patients with cardiac transplants to identify the characteristics of cardiac allograft vasculopathy. Patients with high-grade rejection are more likely than those with mild/no rejection to have thicker

intima (0.34 mm vs. 0.15 mm in the proximal coronary artery segment, p = 0.005), higher prevalence of macrophages (44% vs. 15%, p = 0.05) and a higher prevalence of intimal microchannels (46% vs. 11%, p = 0.02) on OCT (82). Intimal thickness as measured by OCT increases with time since transplantation (83), and OCT enables the identification of early features of cardiac allograft vasculopathy before development of angiographic features (84). Presence of vulnerable plaque features such as TCFA and macrophage infiltration increases with time from transplantation, and complex lesions such as intimal laceration and plaque rupture are also more prevalent (85).

LIMITATIONS OF OCT

A major limitation of OCT is its requirement for a blood-free field, necessitating flushing with either saline or contrast during image acquisition. Any contamination with blood during pullback results in loss of image data due to backscattering. Differentiation of calcium and lipid pool is more challenging than with IVUS, as both give low-attenuation signals (86). Moreover, the limited ranging depth of OCT (5 to 6 mm) means that imaging of the left main stem and vein grafts is limited (13), and calculation of plaque volume may be inaccurate (7). Poor penetration of light through lipid-rich tissue also limits its use in quantifying certain plaque components. Imaging artifacts plague up to a third of OCT images and thrombus obscures the morphology of the underlying lesion. Plaque analysis of OCT images for features of vulnerability is currently performed on a frame-by-frame basis and is therefore time consuming and not feasible in real time in the catheter laboratory, although automated processes for luminal border detection and plaque composition appear promising (87).

CONCLUSIONS

The detailed spatial resolution provided by OCT has allowed detailed in vivo correlation of those histopathological features thought to underlie plaque vulnerability. This has led to greater insight into the prevalence of vulnerable plaques in patients presenting with ACS, particularly in nonculprit vessels. Although there is lack of clinical data to guide the management of vulnerable lesions, a greater understanding of their natural history and temporal response to pharmacological or invasive interventions may help to deepen the understanding of ACS pathophysiology.

REPRINT REQUESTS AND CORRESPONDENCE: Dr. Vijay Kunadian, Institute of Cellular Medicine, Faculty of Medical Sciences, Newcastle University, Third Floor William Leech Building, Newcastle upon Tyne NE2 4HH, United Kingdom. E-mail: vijay.kunadian@newcastle.ac.uk.

REFERENCES

1. Huang D, Swanson EA, Lin CP, et al. Optical coherence tomography. Science 1991;254:1178–81.

2. Jang IK, Bouma BE, Kang DH, et al. Visualization of coronary atherosclerotic plaques in patients using optical coherence tomography: comparison with intravascular ultrasound. J Am Coll Cardiol 2002;39:604–9.

3. Virmani R, Kolodgie FD, Burke AP, Farb A, Schwartz SM. Lessons from sudden coronary death: a comprehensive morphological classification scheme for atherosclerotic lesions. Arterioscler Thromb Vasc Biol 2000;20:1262–75.

4. Brezinski ME, Tearney GJ, Bouma BE, et al. Optical coherence tomography for optical biopsy. Properties and demonstration of vascular pathology. Circulation 1996;93:1206–13.

5. Prati F, Cera M, Ramazzotti V, Imola F, Giudice R, Albertucci M. Safety and feasibility of a new non-occlusive technique for facilitated intracoronary optical coherence tomography (OCT) acquisition in various clinical and anatomical scenarios. EuroIntervention 2007;3:365–70.

6. Choma M, Sarunic M, Yang C, Izatt J. Sensitivity advantage of swept source and Fourier domain optical coherence tomography. Optics Express 2003;11:2183–9.

7. Prati F, Guagliumi G, Mintz GS, et al. Expert review document part 2: methodology, terminology and clinical applications of optical coherence tomography for the assessment of interventional procedures. Eur Heart J 2012;33:2513–20.

8. Tearney GJ, Regar E, Akasaka T, et al. Consensus standards for acquisition, measurement, and reporting of intravascular optical coherence tomography studies: a report from the International Working Group for Intravascular Optical Coherence Tomography Standardization and Validation. J Am Coll Cardiol 2012;59:1058–72.

9. Kume T, Akasaka T, Kawamoto T, et al. Assessment of coronary arterial thrombus by optical coherence tomography. Am J Cardiol 2006;97:1713–7.

10. Yabushita H, Bouma BE, Houser SL, et al. Characterization of human atherosclerosis by optical coherence tomography. Circulation 2002;106:1640–5.

11. Kume T, Akasaka T, Kawamoto T, et al. Assessment of coronary intima–media thickness by optical coherence tomography: comparison with intravascular ultrasound. Circulation J 2005;69:903–7.

12. Motreff P, Levesque S, Souteyrand G, et al. High-resolution coronary imaging by optical coherence tomography: feasibility, pitfalls and artefact analysis. Arch Cardiovasc Dis 2010;103:215–26.

13. Moharram MA, Yeoh T, Lowe HC. Swings and roundabouts: intravascular optical coherence tomography (OCT) in the evaluation of the left main stem coronary artery. Int J Cardiol 2011;148:243–4.

14. Farb A, Burke AP, Tang AL, et al. Coronary plaque erosion without rupture into a lipid core. a frequent cause of coronary thrombosis in sudden coronary death. Circulation 1996;93:1354–63.

15. Burke AP, Farb A, Malcom GT, Liang YH, Smialek J, Virmani R. Coronary risk factors and plaque morphology in men with coronary disease who died suddenly. N Engl J Med 1997;336:1276–82.

16. Schaar JA, Muller JE, Falk E, et al. Terminology for high-risk and vulnerable coronary artery plaques. Report of a meeting on the vulnerable plaque, June 17 and 18, 2003, Santorini, Greece. Eur Heart J 2004;25:1077–82.

17. Tanaka A, Imanishi T, Kitabata H, et al. Morphology of exertion-triggered plaque rupture

in patients with acute coronary syndrome: an optical coherence tomography study. Circulation 2008;118:2368–73.

18. Jang IK, Tearney GJ, MacNeill B, et al. In vivo characterization of coronary atherosclerotic plaque by use of optical coherence tomography. Circulation 2005;111:1551–5.

19. Kubo T, Imanishi T, Kashiwagi M, et al. Multiple coronary lesion instability in patients with acute myocardial infarction as determined by optical coherence tomography. Am J Cardiol 2010;105:318–22.

20. Ino Y, Kubo T, Tanaka A, et al. Difference of culprit lesion morphologies between ST-segment elevation myocardial infarction and non-ST-segment elevation acute coronary syndrome: an optical coherence tomography study. J Am Coll Cardiol Intv 2011;4:76–82.

21. Tian J, Hou J, Xing L, et al. Significance of intraplaque neovascularisation for vulnerability: optical coherence tomography study. Heart 2012;98:1504–9.

22. Kato K, Yonetsu T, Kim SJ, et al. Nonculprit plaques in patients with acute coronary syndromes have more vulnerable features compared with those with non-acute coronary syndromes: a 3-vessel optical coherence tomography study. Circ Cardiovasc Imaging 2012;5:433–40.

23. Tanaka A, Imanishi T, Kitabata H, et al. Distribution and frequency of thin-capped fibroatheromas and ruptured plaques in the entire culprit coronary artery in patients with acute coronary syndrome as determined by optical coherence tomography. Am J Cardiol 2008;102:975–9.

24. Toutouzas K, Karanasos A, Riga M, et al. Optical coherence tomography assessment of the spatial distribution of culprit ruptured plaques and thin-cap fibroatheromas in acute coronary syndrome. EuroIntervention 2012;8:477–85.

25. Toutouzas K, Karanasos A, Tsiamis E, et al. New insights by optical coherence tomography into the differences and similarities of culprit ruptured plaque morphology in non-ST-elevation myocardial infarction and ST-elevation myocardial infarction. Am Heart J 2011;161:1192–9.

26. Zhao Z, Witzenbichler B, Mintz GS, et al. Dynamic nature of nonculprit coronary artery lesion morphology in STEMI: a serial IVUS analysis from the HORIZONS-AMI trial. J Am Coll Cardiol Img 2013;6:86–95.

27. Diletti R, Garcia-Garcia HM, Gomez-Lara J, et al. Assessment of coronary atherosclerosis progression and regression at bifurcations using combined IVUS and OCT. J Am Coll Cardiol Img 2011;4:774–80.

28. Takarada S, Imanishi T, Kubo T, et al. Effect of statin therapy on coronary fibrous-cap thickness in patients with acute coronary syndrome: assessment by optical coherence tomography study. Atherosclerosis 2009;202:491–7.

29. Hattori K, Ozaki Y, Ismail TF, et al. Impact of statin therapy on plaque characteristics as assessed by serial OCT, grayscale and integrated backscatter-IVUS. J Am Coll Cardiol Img 2012;5:169–77.

30. Nishio R, Shinke T, Otake H, et al. Stabilizing effect of combined eicosapentaenoic acid and statin therapy on coronary thin-cap fibroatheroma. Atherosclerosis 2014;234:114–9.

31. Guo J, Chen YD, Tian F, et al. Thrombosis and morphology of plaque rupture using optical coherence tomography. Chin Med J (Engl) 2013;126:1092–5.

32. Vergallo R, Ren X, Yonetsu T, et al. Pancoronary plaque vulnerability in patients with acute coronary syndrome and ruptured culprit plaque: a 3-vessel optical coherence tomography study. Am Heart J 2014;167:59–67.

33. Shimamura K, Ino Y, Kubo T, et al. Difference of ruptured plaque morphology between asymptomatic coronary artery disease and non-ST elevation acute coronary syndrome patients: an optical coherence tomography study. Atherosclerosis 2014;235:532–7.

34. Kubo T, Imanishi T, Takarada S, et al. Assessment of culprit lesion morphology in acute myocardial infarction: ability of optical coherence tomography compared with intravascular ultrasound and coronary angioscopy. J Am Coll Cardiol 2007;50:933–9.

35. Jia H, Abtahian F, Aguirre AD, et al. In vivo diagnosis of plaque erosion and calcified nodule in patients with acute coronary syndrome by intravascular optical coherence tomography. J Am Coll Cardiol 2013;62:1748–58.

36. Ferrante G, Nakano M, Prati F, et al. High levels of systemic myeloperoxidase are associated with coronary plaque erosion in patients with acute coronary syndromes: a clinicopathological study. Circulation 2010;122:2505–13.

37. Prati F, Uemura S, Souteyrand G, et al. OCT-based diagnosis and management of STEMI associated with intact fibrous cap. J Am Coll Cardiol Img 2013;6:283–7.

38. Naghavi M, Libby P, Falk E, et al. From vulnerable plaque to vulnerable patient: a call for new definitions and risk assessment strategies: part I. Circulation 2003;108:1664–72.

39. Mizukoshi M, Kubo T, Takarada S, et al. Coronary superficial and spotty calcium deposits in culprit coronary lesions of acute coronary syndrome as determined by optical coherence tomography. Am J Cardiol 2013;112:34–40.

40. Kato K, Yonetsu T, Kim SJ, et al. Comparison of nonculprit coronary plaque characteristics between patients with and without diabetes: a 3-vessel optical coherence tomography study. J Am Coll Cardiol Intv 2012;5:1150–8.

41. Uemura S, Ishigami K, Soeda T, et al. Thin-cap fibroatheroma and microchannel findings in optical coherence tomography correlate with subsequent progression of coronary atheromatous plaques. Eur Heart J 2012;33:78–85.

42. Moreno PR, Purushothaman KR, Fuster V, et al. Plaque neovascularization is increased in ruptured atherosclerotic lesions of human aorta: implications for plaque vulnerability. Circulation 2004;110:2032–8.

43. Kitabata H, Tanaka A, Kubo T, et al. Relation of microchannel structure identified by optical coherence tomography to plaque vulnerability in patients with coronary artery disease. Am J Cardiol 2010;105:1673–8.

44. Kubo T, Akasaka T, Shite J, et al. OCT compared with IVUS in a coronary lesion assessment: the OPUS-CLASS study. J Am Coll Cardiol Img 2013;6:1095–104.

45. Sawada T, Shite J, Garcia-Garcia HM, et al. Feasibility of combined use of intravascular ultrasound radiofrequency data analysis and optical coherence tomography for detecting thin-cap fibroatheroma. Eur Heart J 2008;29:1136–46.

46. Kubo T, Nakamura N, Matsuo Y, et al. Virtual histology intravascular ultrasound compared with optical coherence tomography for identification of thin-cap fibroatheroma. Int Heart J 2011;52:175–9.

47. Li J, Li X, Jing J, et al. Integrated intravascular optical coherence tomography (OCT) – ultrasound (US) catheter for characterization of atherosclerotic plaques in vivo. Conf Proc IEEE Eng Med Biol Soc 2012;2012:3175–8.

48. Li J, Ma T, Jing J, et al. Miniature optical coherence tomography-ultrasound probe for automatically coregistered three-dimensional intracoronary imaging with real-time display. J Biomed Opt 2013;18:100502.

49. Observational Study of Optical Coherence Tomography (OCT) in Patients Undergoing Fractional Flow Reserve (FFR) and Percutaneous Coronary Intervention (ILUMIEN I). 2014. Available at: https://clinicaltrials.gov/ct2/show/NCT01663896?term=ILUMIEN+I&rank=1. Accessed January 31, 2014.

50. Brugaletta S, Garcia-Garcia HM, Serruys PW, et al. NIRS and IVUS for characterization of atherosclerosis in patients undergoing coronary angiography. J Am Coll Cardiol Img 2011;4:647–55.

51. Maehara A, Mintz GS, Weissman NJ. Advances in intravascular imaging. Circ Cardiovasc Interv 2009;2:482–90.

52. Regar E, Gnanadesigan M, Van der Steen AF, van Soest G. Quantitative optical coherence tomography tissue-type imaging for lipid-core plaque detection. J Am Coll Cardiol Intv 2013;6:891–2.

53. Roleder T, Kovacic JC, Ali Z, et al. Combined NIRS and IVUS imaging detects vulnerable plaque using a single catheter system: a head-to-head comparison with OCT. EuroIntervention 2014;10:303–11.

54. Fard AM, Vacas-Jacques P, Hamidi E, et al. Optical coherence tomography–near infrared spectroscopy system and catheter for intravascular imaging. Optics Express 2013;21:30849–58.

55. Gurmeric S, Isguder GG, Carlier S, Unal G. A new 3-D automated computational method to evaluate in-stent neointimal hyperplasia in in-vivo intravascular optical coherence tomography pullbacks. Med Image Comput Comput Assist Interv 2009;12:776–85.

56. Athanasiou LS, Bourantas CV, Siogkas PK, et al. 3D reconstruction of coronary arteries using frequency domain optical coherence tomography images and biplane angiography. Conf Proc IEEE Eng Med Biol Soc 2012;2012:2647–50.

57. Bourantas CV, Papafaklis MI, Lakkas L, et al. Fusion of optical coherence tomographic and angiographic data for more accurate evaluation of

the endothelial shear stress patterns and neointimal distribution after bioresorbable scaffold implantation: comparison with intravascular ultrasound-derived reconstructions. Int J Cardiovasc Imaging 2014;30:485–94.

58. Fukumoto Y, Hiro T, Fujii T, et al. Localized elevation of shear stress is related to coronary plaque rupture: a 3-dimensional intravascular ultrasound study with in-vivo color mapping of shear stress distribution. J Am Coll Cardiol 2008; 51:645–50.

59. Joshi NV, Vesey AT, Williams MC, et al. 18F-fluoride positron emission tomography for identification of ruptured and high-risk coronary atherosclerotic plaques: a prospective clinical trial. Lancet 2014;383:705–13.

60. Kimura T, Yokoi H, Nakagawa Y, et al. Three-year follow-up after implantation of metallic coronary-artery stents. N Engl J Med 1996;334:561–6.

61. Nakagawa Y, Kimura T, Morimoto T, et al. Incidence and risk factors of late target lesion revascularization after sirolimus-eluting stent implantation (3-year follow-up of the j-Cypher Registry). Am J Cardiol 2010;106:329–36.

62. Kang SJ, Lee CW, Song H, et al. OCT analysis in patients with very late stent thrombosis. J Am Coll Cardiol Img 2013;6:695–703.

63. Takano M, Yamamoto M, Inami S, et al. Appearance of lipid-laden intima and neovascularization after implantation of bare-metal stents extended late-phase observation by intracoronary optical coherence tomography. J Am Coll Cardiol 2009;55:26–32.

64. Kang SJ, Mintz GS, Akasaka T, et al. Optical coherence tomographic analysis of in-stent neoatherosclerosis after drug-eluting stent implantation. Circulation 2011;123:2954–63.

65. Kim JS, Hong MK, Shin DH, et al. Quantitative and qualitative changes in DES-related neointimal tissue based on serial OCT. J Am Coll Cardiol Img 2012;5:1147–55.

66. Yonetsu T, Kato K, Kim SJ, et al. Predictors for neoatherosclerosis: a retrospective observational study from the optical coherence tomography registry. Circ Cardiovasc Imag 2012;5:660–6.

67. Tian F, Chen Y, Liu H, Zhang T, Guo J, Jin Q. Assessment of characteristics of neointimal hyperplasia after drug-eluting stent implantation in patients with diabetes mellitus: an optical coherence tomography analysis. Cardiol 2014;128: 34–40.

68. Lee SY, Shin DH, Mintz GS, et al. Optical coherence tomography-based evaluation of in-stent neoatherosclerosis in lesions with more than 50% neointimal cross-sectional area stenosis. EuroIntervention 2013;9:945–51.

69. Saw J. Coronary angiogram classification of spontaneous coronary artery dissection. Catheter Cardiovasc Interv 2013;84:1115–22.

70. Paulo M, Sandoval J, Lennie V, et al. Combined use of OCT and IVUS in spontaneous coronary artery dissection. J Am Coll Cardiol Img 2013;6: 830–2.

71. Alfonso F, Paulo M, Gonzalo N, et al. Diagnosis of spontaneous coronary artery dissection by optical coherence tomography. J Am Coll Cardiol 2012;59:1073–9.

72. Nishiguchi T, Tanaka A, Ozaki Y, et al. Prevalence of spontaneous coronary artery dissection in patients with acute coronary syndrome. Eur Heart J Acute Cardiovasc Care 2013 Sep 11 [E-pub ahead of print].

73. Park HC, Choi SI, Lee JU, Kim SG, Shin J, Kim HJ. Morphological findings in typical variant angina presenting as acute coronary syndrome using optical coherence tomography. J Interv Cardiol 2013;26:491–500.

74. Morikawa Y, Uemura S, Ishigami K, et al. Morphological features of coronary arteries in patients with coronary spastic angina: assessment with intracoronary optical coherence tomography. Int J Cardiol 2011;146:334–40.

75. Tanaka A, Shimada K, Tearney GJ, et al. Conformational change in coronary artery structure assessed by optical coherence tomography in patients with vasospastic angina. J Am Coll Cardiol 2011;58:1608–13.

76. Sanidas EA, Brener SJ, Maehara A, et al. Outcomes in diabetic patients undergoing primary percutaneous coronary intervention for acute anterior myocardial infarction: results from the INFUSE-AMI study. Catheter Cardiovasc Interv 2014;83:704–10.

77. Chia S, Raffel OC, Takano M, Tearney GJ, Bouma BE, Jang IK. Comparison of coronary plaque characteristics between diabetic and non-diabetic subjects: an in vivo optical coherence tomography study. Diabetes Res Clin Pr 2008;81: 155–60.

78. Feng T, Yundai C, Lian C, et al. Assessment of coronary plaque characteristics by optical coherence tomography in patients with diabetes mellitus complicated with unstable angina pectoris. Atherosclerosis 2010;213:482–5.

79. Niccoli G, Giubilato S, Di Vito L, et al. Severity of coronary atherosclerosis in patients with a first acute coronary event: a diabetes paradox. Eur Heart J 2013;34:729–41.

80. Deo R, Fyr CL, Fried LF, et al. Kidney dysfunction and fatal cardiovascular disease—an association independent of atherosclerotic events: results from the Health, Aging, and Body Composition (Health ABC) study. Am Heart J 2008;155:62–8.

81. Kato K, Yonetsu T, Jia H, et al. Nonculprit coronary plaque characteristics of chronic kidney disease. Circ Cardiovasc Imaging 2013;6:448–56.

82. Dong L, Maehara A, Nazif TM, et al. Optical coherence tomographic evaluation of transplant coronary artery vasculopathy with correlation to cellular rejection. Circ Cardiovasc Interv 2014;7: 199–206.

83. Garrido IP, Garcia-Lara J, Pinar E, et al. Optical coherence tomography and highly sensitivity troponin T for evaluating cardiac allograft vasculopathy. Am J Cardiol 2012;110:655–61.

84. Khandhar SJ, Yamamoto H, Teuteberg JJ, et al. Optical coherence tomography for characterization of cardiac allograft vasculopathy after heart transplantation (OCTCAV study). J Heart Lung Transplant 2013;32:596–602.

85. Cassar A, Matsuo Y, Herrmann J, et al. Coronary atherosclerosis with vulnerable plaque and complicated lesions in transplant recipients: new insight into cardiac allograft vasculopathy by optical coherence tomography. Eur Heart J 2013; 34:2610–7.

86. Manfrini O, Mont E, Leone O, et al. Sources of error and interpretation of plaque morphology by optical coherence tomography. Am J Cardiol 2006;98:156–9.

87. Athanasiou LS, Bourantas CV, Rigas GA, et al. Fully automated calcium detection using optical coherence tomography. Conf Proc IEEE Eng Med Biol Soc 2013;2013:1430–3.

88. Zafar H, Ullah I, Dinneen K, et al. Evaluation of hemodynamically severe coronary stenosis as determined by fractional flow reserve with frequency domain optical coherence tomography measured anatomical parameters. J Cardiol 2014; 64:19–24.

89. Reith S, Battermann S, Jaskolka A, et al. Relationship between optical coherence tomography derived intraluminal and intramural criteria and haemodynamic relevance as determined by fractional flow reserve in intermediate coronary stenoses of patients with type 2 diabetes. Heart 2013;99:700–7.

90. Pyxaras SA, Tu S, Barbato E, et al. Quantitative angiography and optical coherence tomography for the functional assessment of nonobstructive coronary stenoses: comparison with fractional flow reserve. Am Heart J 2013;166:1010–18.e1.

91. Pawlowski T, Prati F, Kulawik T, Ficarra E, Bil J, Gil R. Optical coherence tomography criteria for defining functional severity of intermediate lesions: a comparative study with FFR. Int J Cardiovasc Imag 2013;29:1685–91.

92. Gonzalo N, Escaned J, Alfonso F, et al. Morphometric assessment of coronary stenosis relevance with optical coherence tomography: a comparison with fractional flow reserve and intravascular ultrasound. J Am Coll Cardiol 2012; 59:1080–9.

93. Shiono Y, Kitabata H, Kubo T, et al. Optical coherence tomography-derived anatomical criteria for functionally significant coronary stenosis assessed by fractional flow reserve. Circulation J 2012;76:2218–25.

KEY WORDS acute coronary syndrome, coronary artery disease, intravascular imaging, optical coherence tomography, percutaneous intervention